Indian Journal of Geo Marine Sciences
Vol. 49 (02), February 2020, pp. 175-183

Feature Extraction Method for Ship-Radiated Noise Based on Extreme-point Symmetric Mode Decomposition and Dispersion Entropy

Guohui Li, Ke Zhao & Hong Yang
School of Electronic Engineering, Xi'an University of Posts and Telecommunications, Xi'an, Shaanxi 710 121, China
[E-mail: lghcd@163.com; uestcyhong@163.com]

Received 06 June 2018; revised 14 September 2018

A novel feature extraction method for ship-radiated noise based on extreme-point symmetric mode decomposition (ESMD) and dispersion entropy (DE) is proposed in the present study. Firstly, ship-radiated noise signals were decomposed into a set of band-limited intrinsic mode functions (IMFs) by ESMD. Then, the correlation coefficient (CC) between each IMF and the original signal were calculated. Finally, the IMF with highest CC was selected to calculate DE as the feature vector. Comparing DE of the IMF with highest CC by empirical mode decomposition (EMD), ensemble empirical mode decomposition (EEMD) and ESMD, it is revealed that the proposed method can assist the feature extraction and classification recognition for ship-radiated noise.

[Keywords: Dispersion entropy; Extreme-point symmetric mode decomposition; Feature extraction; Ship-radiated noise]

Introduction

Ship-radiated noise can better reflect the performance of the ship such as speed, type, tonnage, and so on. However, the ocean environment complexity has made it difficult to extract these ship feature[1,2]. The acquisition of ship-radiated noise is the premise of feature extraction. At present, ship-radiated noise is mainly obtained by acoustic measurement technology. The virtual time reversal mirror method can more effectively measure ship-radiated noise[3]. In addition, acoustic measurement can also be used to analyze the polarization status of homogenous/inhomogeneous waves propagating in layered isotropic/anisotropic media[4,5], to verify the existence of acoustic Goos-Hänch effect[6], and so on. The traditional feature extraction of the ship-radiated noise is mainly used to detect the line spectrum feature and signal strength. If the intensity of the ocean background noise is greater than the intensity of the target signal, the reliability of the spectrum analysis method will be significantly reduced. The ship-radiated noise signals have non-stationary and non-Gaussian characteristics after propagating through complex ocean channel. Traditional signal processing algorithms[7-11] cannot deal with these problems effectively. The Fourier transform can only display the frequency domain characteristics, and cannot reflect well the time-varying characteristics of signals. The wavelet transform can provide time-varying characteristics of signals, but it is easily affected by wavelet basis functions and decomposition times.

Empirical mode decomposition (EMD)[12,13] is self-adaptive signal decomposition method which can decompose the signal into a set of intrinsic mode functions (IMFs) with different frequencies. However, the occurrence of mode mixing during decomposition, may lead to unsatisfactory decomposition results. Ensemble empirical mode decomposition (EEMD)[14,15] has been put forward on the basis of EMD. In the EEMD, Gaussian white noise is added into the original signal sequence. The uniform distribution of white noise spectrum has been used to improve the mode mixing problem and the precision of signal decomposition. However, the added white noise in EEMD has caused a series of problems, such as increased computational complexity, slower decomposition speed, and so on. Extreme-point symmetric mode decomposition (ESMD)[16,17] improves the envelope interpolation method on the basis of empirical mode decomposition, which is a good time-frequency processing method. This method has low computational complexity and does not need to introduce redundant noise signals. Therefore, ESMD is introduced to decompose ship-radiated noise.

With the in-depth study of the ESMD, EMD, and EEMD theories, we have found that they can be widely used in the process and analysis of non-stationary, non-linear and non-Gaussian signals in oceanography, atmospheric science, information science, economics, ecology, medicine and seismology[18], such as fault diagnosis[19-21] and underwater acoustic signal processing[22]. A fault diagnosis method of gear vibration signals based on EMD was proposed in 2002[19]. EEMD and Hilbert transform were used to study gearbox fault diagnosis[20]. A study on fault detection of small current system based on ESMD in 2015, showed that ESMD was more suitable to the fault diagnosis than EMD[21]. Li[22] proposed a feature extraction method of ship-radiated noise based on EEMD, which used the highest energy IMF center frequency to distinguish different types of ships. Later on, Wang[18] verified the advantages of ESMD in data analysis. Most of the above studies prove that ESMD method can be applied to feature extraction, and it is better than EMD and EEMD.

Entropy is firstly proposed by Shannon in 1948[23]. Sample entropy (SE) is widely used in image processing[24]. Although SE is powerful, the computation speed is slow. Permutation entropy (PE) only considers the time information in the time series which has advantages of simple calculation, strong anti-noise ability, good robustness, and low computation cost[25,26]. PE does not consider the difference between the average of the margin and amplitude, so it may lose amplitude information[27]. It is widely used in underwater acoustic signal processing[28,29] and fault diagnosis[30] and can be combined with EMD or EEMD to extract signal features[28]. Multi-scale substitution entropy (MPE) is an improvement to PE, and can also be used for feature extraction[29]. In 2017, a fault diagnosis method of rolling bearing based on VMD and PE was proposed[30]. This method is superior to the diagnosis method of combining EMD and PE. In summary, these methods improve the feature extraction performance by improving the modal decomposition, but they still fail to improve the disadvantage that the PE may lose the amplitude information. The introduction of dispersion entropy (DE) can make up for this deficiency. Therefore, the feature extraction method based on ESMD and DE is proposed and applied to the ship-radiated noise and discussed in this paper.

Materials and Methods

ESMD Algorithm

ESMD is the improvement of the EMD algorithm. EMD decomposes the signal into a series of IMFs and residuals. The decomposition process can be simply expressed as:

$$x(t) = \sum_{j-1}^{x} c_j + R \quad \ldots (1)$$

where, R is residuals, c_j is the IMF component.

In the EMD, the outer envelope of the signal is determined by cubic spline interpolation. In the ESMD, the internal curve interpolation and the adjacent and equal endpoints are used as extreme points in signal decomposition. ESMD allows a certain number of residual extremes when the signal is decomposed. The idea of least square method is used to optimize the final residual modality to determine the best sieving coefficient in the decomposition process[31,32]. Compared with EMD, ESMD effectively solves the problem of mode mixing. Its implementation is as follows[31-33]:

(1) Search for all minimum and maximum points of signal Y, and mark these points with $E_i (1 \le i \le n)$.

(2) Connect all adjacent E_i points with line segments. Mark the midpoint of these line segments as $F_i (1 \le i \le n-1)$.

(3) Increase the midpoint of the boundary between the two ends F_0 and F_n in a certain way.

(4) Construct P-interpolation curve $L_1, L_2, \cdots L_P (P \ge 1)$ with n+1 midpoints and calculate their average:

$$L^* = \frac{L_1 + L_2 + \cdots + L_P}{P} \quad \ldots (2)$$

(5) Calculate $Y - L^*$, and repeat the above four steps until $\left|L^*\right| \le \varepsilon$ (where ε is the allowable error), or the number of sieving reaches the preset maximum K. The first modal function M_1 is obtained.

(6) Calculate $Y - M_1$, and repeat the above five steps with the rest to obtain the remaining modal function $M_2, M_3 \cdots$ until the number of agreed poles does not exceed the remaining residue R.

(7) Change the maximum number of screenings K in a finite integer range $[K_{\min}, K_{\max}]$, repeat the above six steps, calculate the variance δ^2 of $Y-R$, and plot the δ/δ_0 and K curves, where δ_0 is the standard deviation of Y.

(8) Search for the minimum value of K for the corresponding δ/δ_0 minimum value in interval $[K_{\min}, K_{\max}]$. Repeat the first six steps with K_0. The IMF component of the best ESMD decomposition is obtained. At the same time, the obtained R is the optimal adaptive global mean curve.

Analysis of Simulation Signal by ESMD

In order to prove the superiority of the ESMD method, the EMD, EEMD and ESMD are used to decompose the simulation signal. The results are shown in Figure 1. The simulation signal is shown in Equation (3):

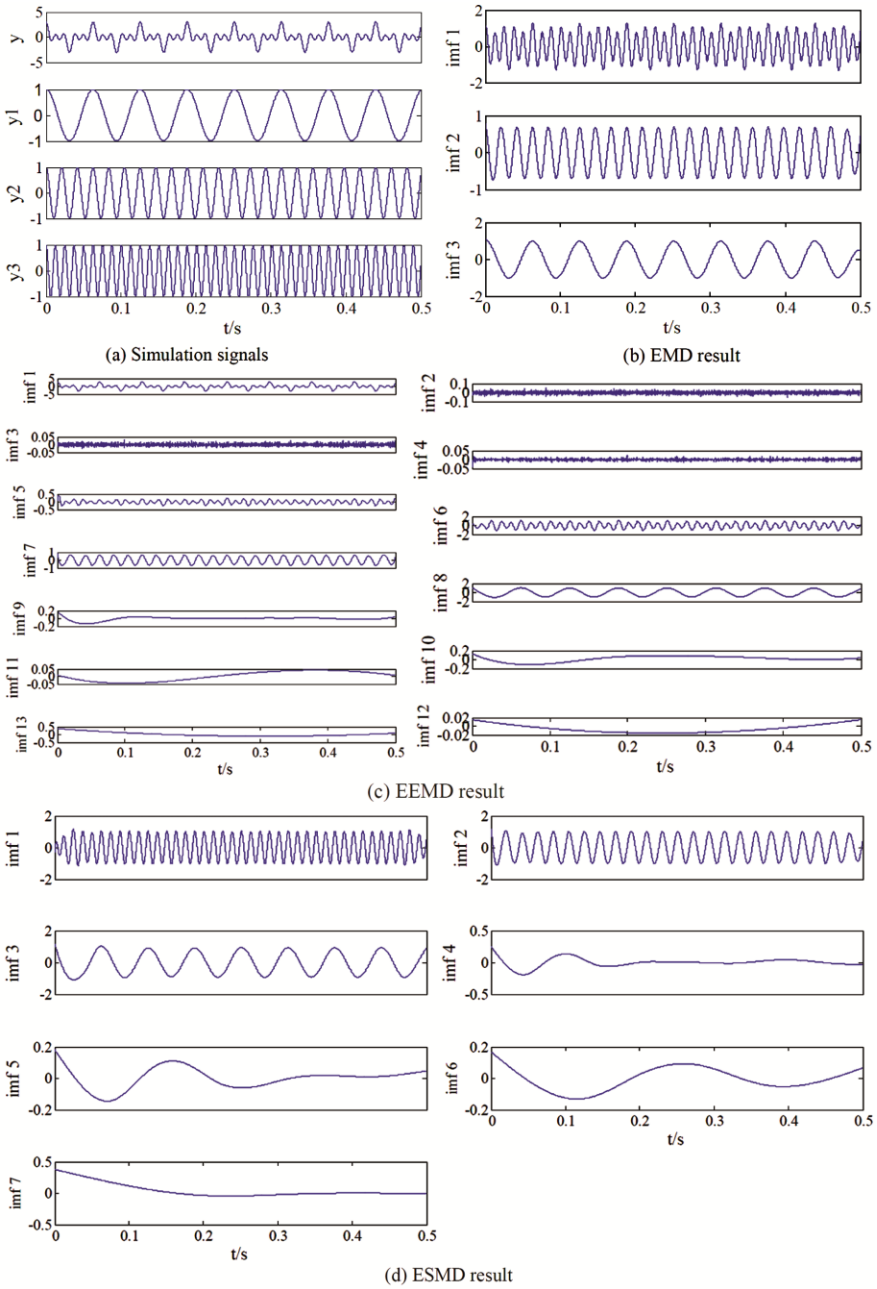

Fig. 1 — The simulation signal and the decomposition result of EMD, EEMD and ESMD

$$\begin{cases} s_1(t) = \cos(100\pi t) \\ s_2(t) = \cos(300\pi t) \\ s_3(t) = \cos(500\pi t) \\ s(t) = s_1(t) + s_2(t) + s_3(t) \end{cases} \quad \ldots (3)$$

where, $s_1(t)$, $s_2(t)$ and $s_3(t)$ respectively represent three components. In Figure 1, the simulation signal is divided into 3 and 13 components by EMD and EEMD respectively. While ESMD divides the simulation signal into 7 components. In Figure 1(b), although the number of IMFs decomposed by EMD is small, there is a significant frequency mixing at IMF1. In Figure 1(c), modal mixing still exists, the noise interference is severe, and EEMD runs slowly. In Figure 1 (d), IMF1, IMF2, IMF3 correspond to y_3, y_2, y_1 in simulation signal. The modal mixing phenomenon is almost absent. In Figure 2, the signal decomposed by EMD, EEMD and ESMD are reconstructed and compared with the original simulation signal. It is found that the recombination of EMD and ESMD coincides with the simulation signal. The signal reconstructed by EEMD is quite different from the original signal. In summary, it is considered that ESMD is better than EMD and EEMD.

DE Algorithm

DE can represent the complexity and irregularity of the signal and is different from PE. It is sensitive to changes in amplitude value, synchronization frequency and time series bandwidth. DE neither need to sort the amplitude value of each embedded vector, nor need to calculate the distance between adjacent embedding dimension, therefore it is very fast[34]. The DE algorithm mainly consists of six steps[34]:

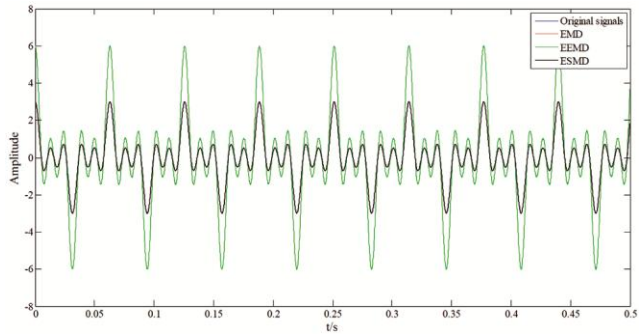

Fig. 2 — Comparison of original signals and signals reconstructed by EMD, EEMD and EMD

(1) For a given sequence $x = x_1, x_2, \cdots x_N$, its length is *N*. Use normal distribution to map $x_j (j = 1, 2, \ldots, N)$ to $y = \{y_j,\ j = 1, 2, \ldots, N\}$, $y_j \in (0, 1)$. The normal distribution function is:

$$y_j = \frac{1}{\sigma\sqrt{2\pi}} \int_{-\infty}^{x_j} e^{\frac{-(t-\mu)^2}{2\sigma^2}} dt \quad \ldots (4)$$

where, μ and σ represent the expectation and standard deviation of the time series, respectively.

(2) Then use the linear transformation to map $z_i^{m,c}$ to the range $[1, 2, \cdots, c]$:

$$z_j^c = round\left(cy_j + 0.5\right) \quad \ldots (5)$$

where, *round* is the integral function, c is the number of categories, and z_j^c is the *j*-th element of the classification time series.

(3) Calculate the embedded vector $z_i^{m,c}$:

$$z_i^{m,c} = \left\{z_i^c, z_{i+d}^c, ..., z_{i+(m-1)d}^c\right\} \quad \ldots (6)$$

where, $i = 1, 2, ..., N - (m-1)d$, m and d represent the embedding dimension and time delay, respectively.

(4) An embedded vector $z_i^{m,c}$ which has an embedding dimension m and time delay d is created according to Equation (6). Each time series $z_i^{m,c}$ is mapped to dispersion mode $\pi_{v_0 v_1 \cdots v_{m-1}}$, where $z_i^c = v_0$, $z_{i+d}^c = v_1, \cdots, z_{i+(m-1)d}^c = v_{m-1}$. Since the signal has m members and each member can be an integer from 1 to c, the possible dispersion pattern that can be assigned to each time series $z_i^{m,c}$ is equal to c^m.

(5) Calculate the probability $p\left(\pi_{v_0, v_1, ..., v_{m-1}}\right)$ of each dispersion pattern $\pi_{v_0, v_1, ..., v_{m-1}}$:

$$p\left(\pi_{v_0, v_1, ..., v_{m-1}}\right) = \frac{N_b\left(\pi_{v_0, v_1, ..., v_{m-1}}\right)}{N - (m-1)d} \quad \ldots (7)$$

where, $N_b\left(\pi_{v_0, v_1, ..., v_{m-1}}\right)$ represents the number of $z_i^{m,c}$ mapped to $\pi_{v_0, v_1, ..., v_{m-1}}$. So $p\left(\pi_{v_0, v_1, ..., v_{m-1}}\right)$ can represent the ratio of the number of $z_i^{m,c}$ mapped to $\pi_{v_0, v_1, ..., v_{m-1}}$.

(6) According to Shannon's definition, the DE of the original time series is:

$$DE(x,m,c,d) = -\sum_{\pi=1}^{c^m} p(r)\ln(p(r)) \quad \ldots (8)$$

$$r = \pi_{v_0,v_1,\ldots,v_{m-1}}$$

where, the embedding dimension m is usually 2 or 3, the number of categories c is an integer between [4, 8], the delay d is generally 1, and the length of the input time series x should be greater than 2000.

From the calculation result, the larger the value of DE, the higher the degree of irregularity of the time series, otherwise the degree of irregularity is lower. From the analysis of the calculation process, when all scatter patterns have the same probability, the data complexity is the highest, and the DE value is the maximum value $\ln(c^m)$. If only one value of $p(\pi_{v_0,v_1,\ldots,v_{m-1}})$ is not zero, it means that the complexity of the time series is the lowest, and DE gets the minimum value.

Simulation Signal Analysis Based on ESMD and DE

The ESMD decomposition of the simulation signal in Equation (3) is shown in Figure 1(d). IMF3, IMF2, and IMF1 correspond to simulation signal s_1, s_2, s_3. Calculate PE, MPE and DE of s_1, s_2, s_3. The results are shown in Table 1. It can be seen from Table 1 that compared with PE and MPE, the DE value after ESMD decomposition is the smallest difference from the DE value of analog signal. Thus the DE method is more stable and accurate than PE and MPE.

Feature Extraction Method Based on ESMD and DE

Choosing a suitable decomposition method is the key to feature extraction. In this paper, ESMD and DE are combined to propose a hybrid feature extraction method. The main steps are as follows:

Table 1 — The PE, MPE and DE of simulation signal and IMF (PE: the embedding dimension is 4, the time delay is 1s; MPE: the embedding dimension is 4, the time delay is 1s, the scale factor is 2; DE: the embedding dimension is 2, the time delay is 1s, and the number of categories is 3)

	Simulation Signal				ESMD Result		
	PE	MPE	DE		PE	MPE	DE
S_1	0.7377	0.7746	1.1058	IMF3	0.7740	0.7374	1.1139
S_2	0.8125	0.9056	1.1641	IMF2	0.8126	0.9055	1.1639
S_3	0.8757	1.0167	1.2112	IMF1	0.8792	1.0198	1.2133

(1) Four types of ship-radiated noise signals are sampled and normalized, then decomposed by ESMD to obtain IMFs.

(2) Calculate the correlation coefficient (CC) between each IMF component and the original signal. Select an IMF component with highest CC with the original signal.

(3) The parameters of DE are determined, and the DE of IMF with highest CC is calculated. The optimal feature is selected as the feature vector which can distinguish four ship-radiated noise signals.

(4) Calculate the DE of 20 samples for each type of ship-radiated noise. Draw the DE diagram to observe whether the feature extraction can be realized.

Feature Extraction of Simulation Signal Based on ESMD and DE

The simulation signal in Equation (9) is used to prove the validity of the proposed method. The simulation signal is as follows:

$$\begin{cases} y_1 = 0.2\cos(50t) \\ y_2 = 0.6\cos(80t) \\ y_3 = \cos(110t) \\ s_1 = y_1 + y_2 + y_3 \\ s_2 = s_1 + n \end{cases} \quad \ldots (9)$$

where, y_1, y_2 and y_3 are three components, n is Gaussian white noise, the sampling frequency and the data length are 1 kHz and 1000, respectively. The simulation signal is decomposed using EMD, EEMD and ESMD, as shown in Figure 3.

The DE of IMF with Highest CC

As shown in Figure 3 (a), the modal decomposition of the simulation signal in Equation (9) has been performed. The CC between each IMF and the original simulation signal is calculated. The IMF with highest CC is extracted, and its DE is calculated. The results are shown in Table 2. Observing Table 2, it can be seen that DE with highest CC in the ESMD is more accurate than EMD and EEMD.

Table 2 — The DE of IMF with highest CC in different methods (DE: the embedding dimension, the time delay and the number of categories are 2, 1s and 3, respectively)

	S_2	EMD	EEMD	ESMD
DE	1.6535	1.1969	1.2606	1.8997

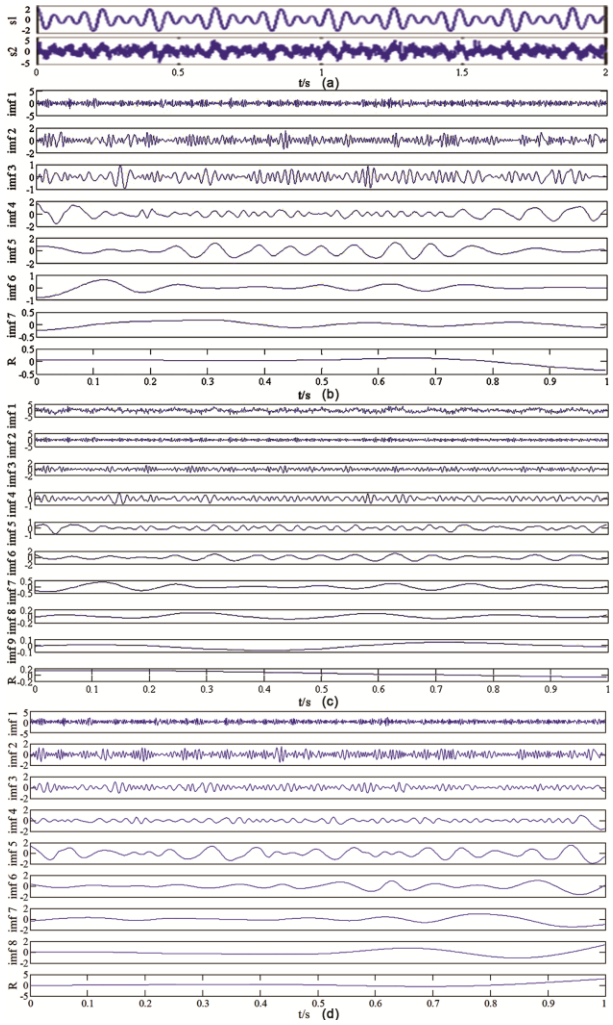

Fig. 3 — Simulation signal and the decomposition result of EMD, EEMD and ESMD

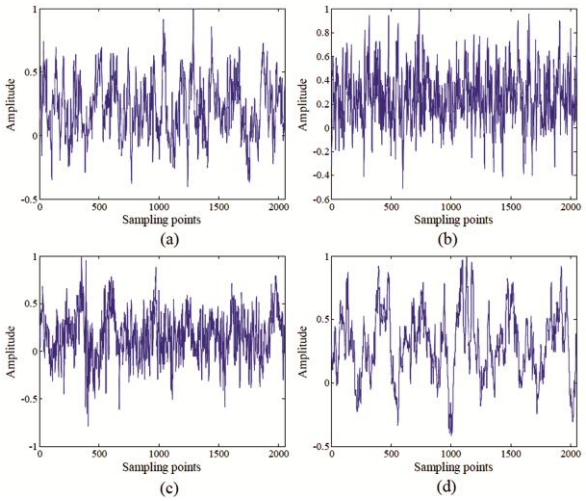

Fig. 4 — The time domain waveform of four types of ship-radiated noise (a) the first type, (b) the second type, (c) the third type and (d) the fourth type

Result and Discussion

The ESMD of Ship-radiated Noise

Four types of ship-radiated noise signals were selected, as shown in Figure 4. The sampling rate is 20KHz, and the data length is 2048. The four types of signals are normalized. The normalized sample is decomposed into IMFs using ESMD, as shown in Figure 5.

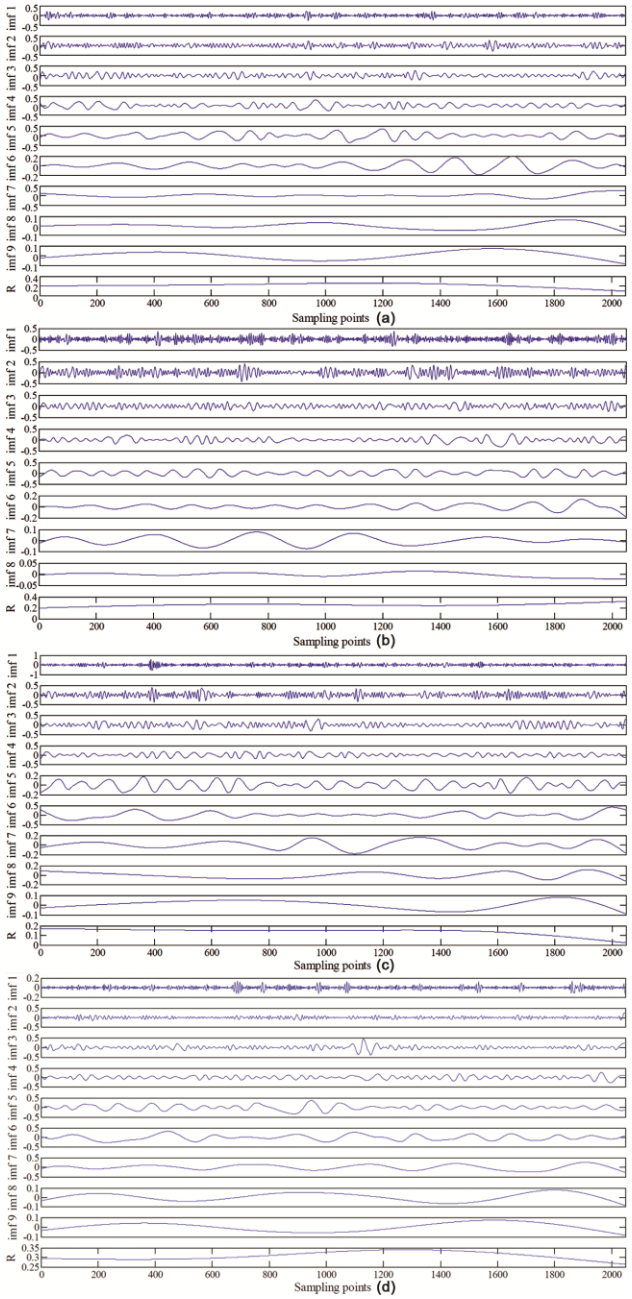

Fig. 5 — The results of ESMD of four types of ship-radiated noise: (a) the first type, (b) the second type, (c) the third type and (d) the fourth type

Feature Extraction of Ship-Radiated Noise

According to the ESMD decomposition results for four types of ship-radiated noise signals, the IMF with highest CC can be obtained. The results are shown in Table 3. For each type of ship-radiated noise signal, 20 samples were selected randomly to calculate the DE as the feature vector. The DE distribution of four types of ship-radiated noise is shown in Figure 6. Due to the presence of marine background noise, DE can only distinguish the radiated noise of the fourth category of ships, and the other three categories cannot be distinguished. For comparison, the DE with highest CC was calculated after the decomposition of EMD and EEMD, as shown in Figure 7 and Figure 8. The PE, MPE and DE of the IMF with highest CC after ESMD decomposition are shown in Figures 9-11.

In Figures 6-8 and 11, the embedding dimension is 2, the time delay is 1s, and the number of categories is 3. In Figure 9, the embedding dimension is 4, and the time delay is 1s. In Figure 10, the embedding dimension is 4, the delay time is 1s, and the scale factor is 2. It can be seen from Figure 7 that third and fourth types of signals are indistinguishable. In Figure 8, first and fourth types of signals are indistinguishable. In Figure 9 and Figure 10, four types of signals cannot be distinguished completely. In Figure 11, four types of signals can be

Table 3 — The highest CC of IMF after ESMD decomposition

	The First Type	The Second Type	The Third Type	The Fourth Type
IMF	5	2	6	6

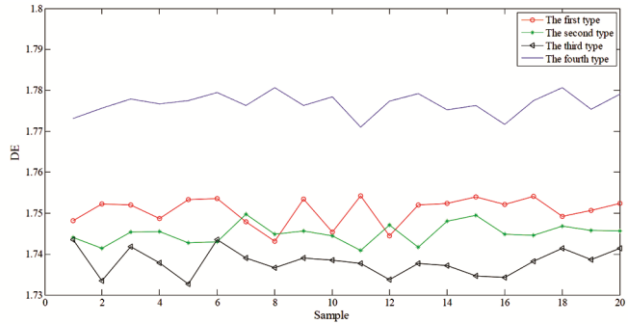

Fig. 6 — The DE distribution of four types of ship-radiated noise

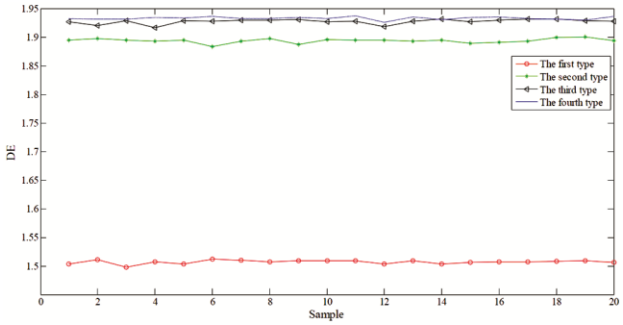

Fig. 7 — The DE distribution of IMF with highest CC by EMD

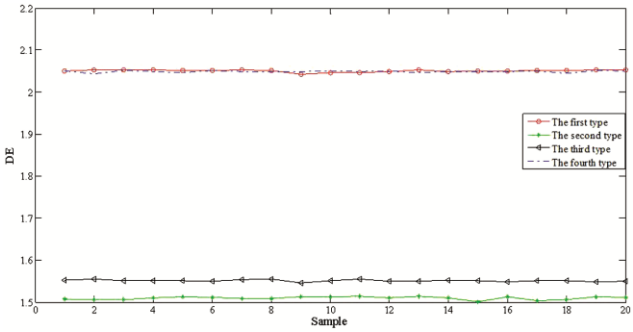

Fig. 8 — The DE distribution of IMF with highest CC by EEMD

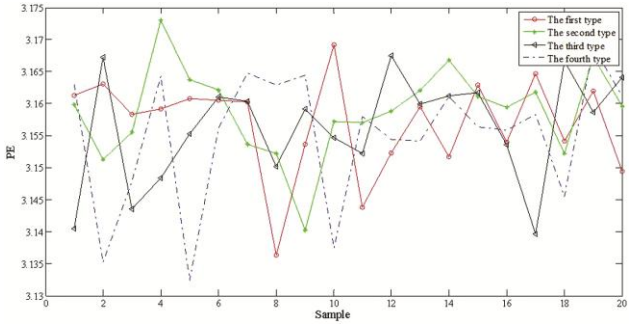

Fig. 9 — The PE distribution of IMF with highest CC by ESMD

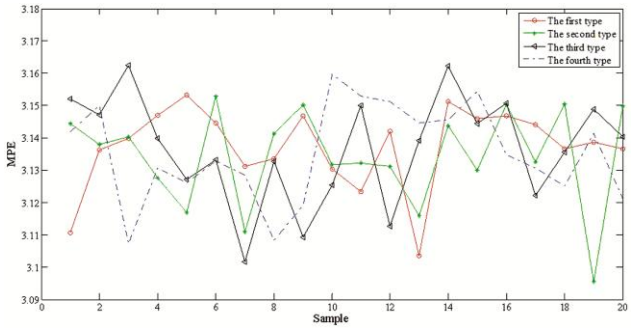

Fig. 10 — The MPE distribution of IMF with highest CC by ESMD

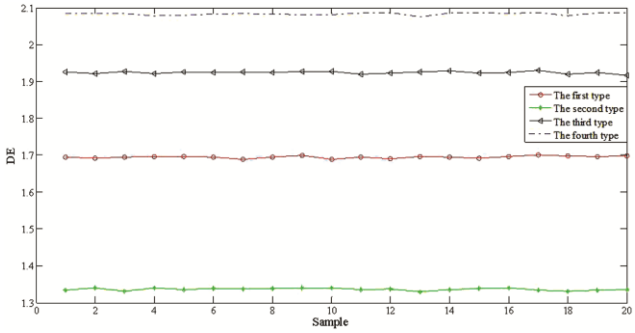

Fig. 11 — The DE distribution of IMF with highest CC by ESMD

distinguished clearly. In summary, the DE value of the IMF component with highest CC after ESMD decomposition has good separability.

Conclusion

This paper proposes a new feature extraction method, which can distinguish ship-radiated noise signals by combining ESMD and DE. ESMD is used to decompose four types of ship-radiated noise signals, and extracts the IMF with highest CC. The DE of the IMF with highest CC is calculated as the feature vector which is used to distinguish four types of signals. This article proves the effectiveness and superiority of the method through experiments. This method has the following advantages:

(1) Compared to the method proposed by Li[28], this paper uses ESMD instead of EMD. The simulation results show that the decomposition effect of the ESMD method is more accurate than EMD and EEMD. ESMD solves the problem of frequency aliasing in the EMD.

(2) Compared to the method proposed by Li[28], this paper uses DE instead of PE. PE does not consider the difference between the average amplitude and the amplitude. It may lose amplitude information, but DE can compensate for this shortcoming. It has confirmed that DE is more stable than PE and MPE. DE can be used to extract features of different types of ship-radiated noise signals.

(3) We compared the DE of the IMF with highest CC after the decomposition of EMD and EEMD, and the PE, MPE and DE of the IMF with highest CC after the decomposition of ESMD. Finally, it is proved that the method has better separability.

Acknowledgment

This work was supported by the National Natural Science Foundation of China (No. 51709228).

References

1 Li, Y. X., Li, Y. A., Chen, X. & Yu J., A feature extraction method of ship-radiated noise based on sample entropy and ensemble empirical mode decomposition. *J. Unmanned Undersea Sys.*, 26 (1) (2018): 28-34.

2 Wang, P. P., Zhang, G. J., Guan, L. G. & Wang, P., The method research of extracting the characteristic line spectrum from the ship-radiated noise. *Ocean Technol.*, 29 (3) (2010): 47-50.

3 Xiang, L. F., Sun, C., Liu, Z. W. & Du, J. Y., Measuring ship-radiated noise level via vertical linear array based on virtual time reversal mirror. *Chinese J. Acous.*, 38 (1) (2013): 57-64.

4 Fa, L., Zhao, J., Han, Y. L., Li, G. H., Ding, P. F. & Zhao, M. S., The influence of rock anisotropy on elliptical-polarization state of inhomogenously refracted P-wave. *Science China Phys. Mech.*, 59 (4) (2016): 644301(1-7).

5 Fa, L., Li, W. Y., Zhao, J., Han, Y. L., Liang, M., Ding, P. F. & Zhao, M. S., Polarization state of an inhomogenously refracted compressional-wave induced at interface between two anisotropic rocks. *J. Acous. Soc. America*, 141 (1) (2017): 1-6.

6 Fa, L., Xue, L., Fa, Y. X., Han, Y. L., Zhang, Y. D., Cheng, H. S., Ding, P. F., Li, G. H., Tang, S. J., Bai, C. L., Xi, B. J., Zhang, X. L. & Zhao, M. S., Acoustic Goos-Hänchen effect. *Science China Phys. Mech.*, 60 (10) (2017): 104311(1-12).

7 Fan, Y. Y., Shang, J. H., Sun, J. C., Li, P. G. & Xu, J. D., Feature extraction of ship-radiated noise using higher-order spectrum. *Chin. J. Acoust.*, 19 (2) (2000): 159-165.

8 Zeng, Z. L., Li, Y. A. & Liu, X. H., Study on feature extraction of ship radiated noise based on higher order spectrum and cepstrum. *Comput. Simul.*, 28 (11) (2011): 5-9.

9 Yan, J. Q., Sun, H. X., Chen, H. L., Naveed, U. R. J. & Cheng, E., Resonance-based time-frequency manifold for feature extraction of ship-radiated noise. *Sensors*, 18 (4) (2018): 936(1-21).

10 Ding, B. J. & Bai, Y. H., Feature extraction of ship radiated noise based on short-time Fourier transform. *Mine Warf. Ship Self-Def.*, 23 (1) (2015): 22-24.

11 Wang, S. G. & Zeng, X. Y., Robust underwater noise targets classification using auditory inspired time-frequency analysis. *Appl. Acoust.*, 78 (2014): 68-76.

12 Wang, Y., Ding, Y. Y., Luo, Q. Z. & Miao, Q. L., Application of EMD and wavelet method to sunspot data. *Int. Conf. Inform. Sci. Technol.*, (2011): 676-678.

13 Boudraa, A. O. & Cexus, J. C., EMD-based signal filtering. *IEEE T. Instrum. Meas.*, 56 (6) (2007): 2196-2202.

14 Lai, Y. Y., Zhang, Z. B., Li, P. Y., Liu, X. L., Liu, Y. X., Xin, Y. & Gu, W. J., Investigation of glucose fluctuations by approaches of multi-scale analysis. *Med. Biol. Eng. Comput.*, 56 (3) (2018): 505-514.

15 Wang, T., Zhang, M. C., Yu, Q. H. & Zhang, H. Y., Comparing the applications of EMD and EEMD on time-frequency analysis of seismic signal. *J. Appl. Geophys.*, 83 (2012), 29-34.

16 Li, H. F., Wang, J. L. & Li, Z. J., Application of ESMD method to air-sea flux investigation. *Int. J. Geosci.*, 4 (5) (2013): 8-11.

17 Lei, J. R., Liu, Z. H., Bai, L., Chen, Z. S., Xu, J. H. & Wang, L. L., The regional features of precipitation variation trends over Sichuan in China by the ESMD method. *Mausam*, 67 (4) (2016): 849-860.

18 Wang, J. L. & Li, Z. J., The ESMD method for climate data analysis. *Clim. Change Res. Let.*, 3 (2014): 1-5.

19 Yu, D. J. & Cheng, J. S., Application of empirical mode decomposition method to gear fault diagnosis. *J. Hunan Univ.*: *Nat. Sci. ed.*, 29 (6) (2002): 48-51.

20 Lin, J. S., Gearbox fault diagnosis based on EEMD and Hilbert transform. *Mech. Transm.*, 34 (5) (2010): 62-64, 75.

21 Wang, Z., Yuan, H. X., Zhang, J. & Yin, Z. H., A new fault line selection method for small current system based on ESMD. *Mech. Electr. Inform.*, (18) (2015): 126-127.

22 Li, Y. X., Li, Y. A. & Chen, X., Ships' radiated noise feature extraction based on EEMD. *J. Vib. Shock*, 36 (5) (2017): 114-119.

23 Shannon, C. E., A mathematical theory of communication. *Bell Sys. Tech. J.*, 27 (3) (1948): 379-423.

24 Liu, D., Zhou, X. Y., Ai, B., Guan, K. & Li, N., Evaluating the flickering complexity of the stored red blood cells using an efficient image processing method. *J. B. Jiaotong Univ.*, 40 (1) (2016): 92-100.

25 Zhu, S. L. & Gan, L., A chaotic signal detection method based on the component permutation of the incomplete two-dimensional phase-space. *Acta Phys. Sin.*, 65 (7) (2016): 070502(1-9).

26 Cao, Y. H., Tung, W. W., Gao, J. B., Protopopescu, V. A. & Hively, L. M., Detecting dynamical changes in time series using the permutation entropy. *Phys. Rev. E*, 70 (4) (2004): 046217(1-7).

27 Zanin, M., Zunino, L., Rosso, O. A. & Papo, D., Permutation entropy and its main biomedical and econophysics applications: a review. *Entropy*, 14 (8) (2012): 1553-1577.

28 Li, Y. X., Li, Y. A., Chen, Z. & Chen, X., Feature extraction of ship-radiated noise based on permutation entropy of the intrinsic mode function with the highest energy. *Entropy*, 18 (11) (2016): 393(1-15).

29 Li, Y. X., Li, Y. A., Chen, X. & Yu, J., A novel feature extraction method for ship-radiated noise based on variational mode decomposition and multi-scale permutation entropy. *Entropy*, 19 (7) (2017): 342(1-16).

30 Zheng, X. X., Zhou, G. W., Ren, H. H. & Fu, Y., A rolling bearing fault diagnosis method based on variational mode decomposition and permutation entropy. *J. Vib. Shock*, 36 (22) (2017): 22-28.

31 Zhang, S. Q., Xu, J. T., Jiang, A. Q., Li, J. F., Su, X. S. & Jiang, W. L., Fault diagnosis of bearings based on extreme-point symmetric mode decomposition and probabilistic neural network. *China Mech. Eng.*, 28 (4) (2017): 425-431.

32 Zhao, Z. & Xu, H., The research of temperature variation trends over Xinjiang in China by extreme-point symmetric mode decomposition method. *Geogr. Res.*, 33(12) (2014): 2358-2366.

33 Li, G. H., Wang, S. L. & Yang, H., Prediction of underwater acoustic signals based on ESMD and ELM. *Indian J. Geo-Mar. Sci.*, 48 (3) (2019): 357-362.

34 Rostaghi, M. & Azami, H., Dispersion entropy: a measure for time series analysis. *IEEE Signal Proc. Let.*, 23 (5) (2016): 610-614.